Environmental Science & Technology

Article

pubs.acs.org/est

Characterizing the Aging of Biomass Burning Organic Aerosol by Use of Mixing Ratios: A Meta-analysis of Four Regions

Matthew D. Jolleys,*[,†] Hugh Coe,[†] Gordon McFiggans,[†] Gerard Capes,[†] James D. Allan,[†,‡] Jonathan Crosier,[†,‡] Paul I. Williams,[†,‡] Grant Allen,[†] Keith N. Bower,[†] Jose L. Jimenez,[§] Lynn M. Russell,[∥] Michel Grutter,[⊥] and Darrel Baumgardner[⊥]

[†]Centre for Atmospheric Science, School of Earth, Atmospheric and Environmental Science, and [‡]National Centre for Atmospheric Science, University of Manchester, Manchester, United Kingdom

[§]Cooperative Institute of Research in the Environmental Sciences and Department of Chemistry and Biochemistry, University of Colorado, Boulder, Colorado, United States

[∥]Scripps Institution of Oceanography, University of California San Diego, La Jolla, California, United States

[⊥]Centro de Ciencias de la Atmósfera, Universidad Nacional Autónoma de México, Mexico City, Mexico

Supporting Information

ABSTRACT: Characteristic organic aerosol (OA) emission ratios (ERs) and normalized excess mixing ratios (NEMRs) for biomass burning (BB) events have been calculated from ambient measurements recorded during four field campaigns. Normalized OA mass concentrations measured using Aerodyne Research Inc. quadrupole aerosol mass spectrometers (Q-AMS) reveal a systematic variation in average values between different geographical regions. For each region, a consistent, characteristic ratio is seemingly established when measurements are collated from plumes of all ages and origins. However, there is evidence of strong regional and local-scale variability between separate measurement periods throughout the tropical, subtropical, and boreal environments studied. ERs close to source typically exceed NEMRs in the far-field, despite apparent compositional change and increasing oxidation with age. The absence of any significant downwind mass enhancement suggests no regional net source of secondary organic aerosol (SOA) from atmospheric aging of BB sources, in contrast with the substantial levels of net SOA formation associated with urban sources. A consistent trend of moderately reduced ΔOA/ΔCO ratios with aging indicates a small net loss of OA, likely as a result of the evaporation of organic material from initial fire emissions. Variability in ERs close to source is shown to substantially exceed the magnitude of any changes between fresh and aged OA, emphasizing the importance of fuel and combustion conditions in determining OA loadings from biomass burning.

1. INTRODUCTION

Biomass burning represents a significant source of organic aerosol (OA) on a global scale, forming an important influence on climate through perturbations to Earth's solar radiation balance. Around 90% of total global primary organic aerosol (POA) is derived from wildfires, prescribed burns, and biofuel combustion, which contribute toward the overall biomass burning (BB) emissions source.[1] The physical and chemical properties of biomass burning organic aerosol (BBOA) and the geographical distribution of fires act to increase the potential for radiative forcing. Sources in tropical regions account for 80% of global BBOA emissions,[2] providing a significant potential radiative forcing given the elevated levels of solar irradiance in the tropics. Eighty to ninety percent of BBOA is in the optically active accumulation mode,[3] a significant fraction of which (45−75%) is highly water-soluble and hence important in promoting cloud droplet formation through increased cloud condensation nuclei (CCN) availability.[4] While efforts have been made to quantify overall source inventories,[5] the fundamental difficulty of prediction of biomass burning emissions exacerbates the uncertainty in these assessments. A critical element of this uncertainty relates to the evolution of aerosol loadings within the atmosphere. In addition to an increase in overall aerosol loadings, secondary formation also acts to increase the single scattering albedo for BB aerosols,[6−8] potentially changing the sign of the resulting climate forcing and presenting a significant uncertainty with regard to the direct radiative effect. While secondary organic aerosol (SOA) formation leading to significant additional OA mass has been widely observed in anthropogenic urban emissions, its net contribution in aging biomass burning plumes remains unclear.[9,10]

Several parameters can be used to characterize biomass burning emissions with respect to source conditions. Emission ratios (ERs) and normalized excess mixing ratios (NEMRs) represent the concentration of an emitted species relative to that of a coemitted reference species,[11,12] with the two definitions applied separately to measurements in the near and far field,

Received: June 14, 2012
Revised: November 6, 2012
Accepted: November 19, 2012
Published: November 19, 2012

respectively. This reference species is typically a nonreactive, conserved gas such as CO or CO_2, expressed as an excess concentration above atmospheric background levels. The ER and NEMR for OA are defined as follows:

$$ER_{OA} = \frac{\Delta OA_{source}}{\Delta CO_{source}} \quad (1)$$

$$NEMR_{OA} = \frac{\Delta OA_{farfield}}{\Delta CO_{farfield}} \quad (2)$$

where ΔOA and ΔCO are the excess OA and CO concentrations, with the latter used in preference to CO_2 due to the greater relative difference with respect to background concentrations. Given that the atmospheric CO lifetime of around 1 month[13] exceeds that of OA (of the order of days to weeks), any reduction in CO concentration over the time scales of several days relevant to the study of BB plumes is primarily limited to the effects of dispersion. The concurrent effect of dispersion on OA concentrations means that any changes in the ΔOA/ΔCO ratio with aging are expected to be dominated by changes to OA in the absence of extensive secondary sources or sinks of CO. The ΔOA/ΔCO ratio can therefore be used as an indicator of OA processing, and specifically SOA formation, which would cause the ratio to increase as OA mass is added in the absence of any coincident enhancement of CO. Throughout this paper, ERs and NEMRs are expressed as dimensionless mass ratios, with both ΔOA and ΔCO concentrations given in units of micrograms per cubic meter at standard temperature and pressure (STP; 273 K, 1 atm). This gives a lower value than ratios expressed in the alternative form of micrograms per cubic meter of OA/parts per million (ppm) of CO. Where necessary, conversion of literature values for comparison was performed in accordance with the ideal gas law at STP.

Emission factors (EFs) provide an alternative means of characterizing biomass burning emissions, relating the amount of a given combustion product to the mass of dry fuel consumed, such that:

$$EF_{OA} = \frac{m_{OA}}{m_{biomass}} = \frac{m_{OA}}{\Delta CO + \Delta CO_2 + \Delta CH_4 + \Delta NMHC + \Delta PM_C} x_c \quad (3)$$

where ΔCO_2, ΔCH_4, ΔNMHC, and ΔPM_C are the masses of C in CO_2, CH_4, all remaining gaseous nonmethane hydrocarbons, and particulate matter, respectively, and x_c is the fuel carbon mass fraction.[14,15] Where the mass of fuel burnt in a fire is not accurately known, fuel consumption can be approximated to the total emitted mass of carbonaceous species. Conversely, in areas where emissions have not been explicitly measured but fire budgets are well-known, a combination of representative EFs and fuel consumption can be used to estimate OA production.

The prevalence of SOA in areas influenced by anthropogenic emissions is well-documented.[9,16] Compiling data from an array of campaigns based in and around urban environments, Zhang et al.[17] showed that SOA constitutes an increasing proportion of total organic particulate mass with increasing distance from source for the urban, urban downwind, and remote sites studied. De Gouw and Jimenez[9] also demonstrate the use of NEMRs to reflect OA aging in urban plumes, highlighting the elevation in ΔOA/ΔCO for measurements of combined POA and SOA above those of POA alone. Initial primary ERs are invariably shown to increase by up to an order of magnitude following addition of SOA. However, no such trend is observed consistently for aging biomass burning emissions. Previous assessments of ambient BBOA have identified both increasing[6,18,19] and decreasing[20] ΔOA/ΔCO with aging, while other studies suggest little or no net change in ΔOA/ΔCO during aging regardless of physical and chemical changes to OA.[21,22] Cubison et al.[22] recently summarized published field measurements of the evolution of ΔOA/ΔCO from BB with aging and reported the potential for a net source of SOA equivalent to 5% of the total global source, albeit with significant statistical uncertainty, encompassing scenarios of no net SOA formation.

This uncertainty in the extent of SOA formation from biomass burning undermines attempts to parametrize the overall effect of aging on aerosol loadings, therefore limiting model prediction of the effects of OA from biomass burning on the climate system. This paper aims to assess the extent of SOA formation in biomass burning plumes by bringing together ERs and NEMRs derived from several different field observations in a range of different biomass burning environments and placing these findings in the context of wider assessments of BBOA emissions and evolution, providing a broader characterization of biomass burning as an aerosol source.

2. DATA SELECTION

A screening procedure was applied to all data in order to isolate those time periods subject to a biomass burning influence, as identifying individual plumes manually would have led to an element of subjectivity in the analysis. Minimum thresholds of ΔCO, number concentration, and f_{60} [ratio of the mass fragment at m/z (mass-to-charge ratio) 60 to the total OA signal] were used to define biomass burning influence, as outlined by Capes et al.[21] The m/z 60 fragment is used as a marker for biomass burning because it is associated with anhydrous sugars such as levoglucosan and related species[23−25] produced by the pyrolysis of plant material, particularly cellulose.[26] An f_{60} threshold of 0.3% was applied, in accordance with background f_{60} levels widely identified in ambient ΔOA measurements,[22] together with minimum ΔCO and number concentrations of 20 ppb and 1000 cm^{-3}, respectively. Minimum observed concentrations for relevant species throughout each individual measurement period were taken as the background values used to determine excess concentrations, with a single background used for the duration of each period. Average ΔOA/ΔCO values were then determined from the fit coefficients for ΔOA versus ΔCO plots for data conforming to these screening criteria from each day or flight (Figure S1, Supporting Information), by use of linear regressions given the larger uncertainties in ΔOA compared to ΔCO. Data were also collated to provide a campaign-wide, regional characteristic ΔOA/ΔCO, while the range of daily/flight average values gave an indication of the extent of variability in ΔOA/ΔCO.

In order to investigate changes in ΔOA/ΔCO with age, data were segregated into fresh and aged fractions. Fresh BB plumes were isolated by identifying peaks in ΔOA concentrations in all time series, where ΔOA concentrations throughout a peak were at least 50% higher than the mean value calculated across the full extent of the given flight or day. Peak selections were then checked for agreement with corresponding reductions of 50% below the mean value in $\Delta O_3/\Delta CO$ time series; this ratio was used as an indicator of aerosol aging, given that the production of O_3 is strongly associated with the photochemical activity that may be expected to be involved in the processing of OA in the

Table 1. ΔOA/ΔCO Coefficients[a]

	ΔOA/ΔCO				
	campaign avg	lowest flight/daily avg	highest flight/daily avg	range	max/min ratio
		ACTIVE			
all data	0.293 ± 0.006	0.203 ± 0.016 (AD09)	0.489 ± 0.013 (SD06)	0.286	2.41
fresh OA	0.329 ± 0.023	0.238 ± 0.013 (SD07)	0.520 ± 0.030 (SD06)	0.282	2.18
aged OA	0.251 ± 0.005	0.203 ± 0.016 (AD09)	0.290 ± 0.008 (AD03)	0.087	1.43
		MILAGRO			
all data	0.049 ± 0.001	0.022 ± 0.003 (01/03/06)	0.090 ± 0.006 (17/03/06)	0.068	4.08
fresh OA	0.051 ± 0.001	0.035 ± 0.010 (10/03/06)	0.070 ± 0.014 (08/03/06)	0.035	1.98
aged OA	0.041 ± 0.001	0.022 ± 0.003 (01/03/06)	0.090 ± 0.003 (17/03/06)	0.068	4.08
		DABEX			
all data	0.056 ± 0.001	0.022 ± 0.002 (B168)	0.071 ± 0.003 (B166)	0.049	3.18
fresh OA	0.065 ± 0.002	0.052 ± 0.003 (B157)	0.080 ± 0.008 (B162)	0.028	1.54
aged OA	0.043 ± 0.001	0.022 ± 0.002 (B168)	0.054 ± 0.001 (B158)	0.031	2.41
		ITOP			
all data	0.019 ± 0.002	0.015 ± 0.002 (B032)	0.054 ± 0.005 (B038)	0.039	2.91

[a]Derived from linear regressions for full campaign data sets, along with segregated fresh and aged OA fractions, with standard deviations of 1σ. Entries in parentheses denote flight numbers and dates corresponding to stated maximum and minimum values.

atmosphere.[27,28] These classifications were further corroborated against concurrent increases in ΔCO and number concentrations, with data fulfilling all criteria designated as fresh OA. While the use of additional aging tracers would have further refined the classification of aerosol ages, wider gas-phase measurements were not consistently performed across all campaigns, preventing intercomparison of this approach between regions and therefore compromising the main aim of this analysis.

3. RESULTS AND DISCUSSION

A series of four ambient biomass burning data sets were included within this meta-analysis, with the aim of characterizing OA emissions and transformations across a number of different regions representing boreal and tropical forests and subtropical grasslands. These data sets are derived from deployments carried out between 2004 and 2006, involving aircraft and ground-based measurements. During the ACTIVE (Aerosol and Chemical Transport in Tropical Convection) campaign, measurements were performed onboard the NERC Dornier-228 aircraft in northern Australia. Other airborne data sets included within this analysis were obtained from two campaigns involving the FAAM (Facility for Airborne Atmospheric Measurements) BAe-146. DABEX (Dust and Biomass Experiment) took place in western Africa, targeting wildfires throughout the region, while ITOP (Intercontinental Transport of Ozone and Precursors) involved the study of highly aged boreal forest fire plumes around the Azores. As part of the wider MILAGRO (Megacities Initiative: Local and Global Research Observations) project, emissions from biomass fires were measured at a ground site at Altzomoni, to the southeast of Mexico City. In each case, total OA mass concentrations were obtained by use of an Aerodyne quadrupole aerosol mass spectrometer (Q-AMS). CO mixing ratios were measured by an Aerolaser AL5002 UV fluorescence CO analyzer on all aircraft campaigns, with both CO and CO_2 measured by a long-path Fourier transform infrared spectrometer at the MILAGRO ground site. Further descriptions of campaigns and instrumentation are provided in the Supporting Information.

A high degree of variability exists in both ERs and NEMRs from biomass burning events. Analysis of ambient aerosol populations influenced by biomass fires from a number of environments demonstrates these differences over a range of temporal and spatial scales, showing significant contrasts in ΔOA/ΔCO both between different regions and between separate fires within a region. Instantaneous ΔOA/ΔCO values cover a range exceeding 2 orders of magnitude, with an overall mean and standard deviation across all campaigns of 0.079 ± 0.078. Representative campaign-averaged ΔOA/ΔCO ratios were calculated by use of regressions incorporating all data points meeting the outlined selection procedure. While the characteristic ratios derived for MILAGRO (0.049 ± 0.001, where the statistical uncertainty associated with fit coefficients is ±1σ) and DABEX (0.056 ± 0.001) are similar, the ratio from ACTIVE (0.293 ± 0.006) is higher by around a factor of 5, illustrating the contrasting nature of emissions originating from different fire locations and mixing of fresh and aged BB airmasses (Table 1). Flight-averaged ΔOA/ΔCO ratios throughout ACTIVE consistently exceeded average ratios from MILAGRO and DABEX by at least a factor of 3 and in some instances by up to an order of magnitude. The lowest flight-averaged ratio derived from the eight ACTIVE flights targeting biomass burning emissions remained more than double the highest examples from any other campaign.

Observed ranges between minimum and maximum flight-averaged, or daily-averaged, values are used to give an indication of the levels of variability in ΔOA/ΔCO between separate sampling periods within each region. A range of 0.286 was identified throughout ACTIVE, exceeding those from MILAGRO (0.068) and DABEX (0.049) by a considerable margin. However, reporting each range as a percentage of its corresponding overall campaign average also accounts for the large contrasts between campaigns and the greater potential for variability where ΔOA/ΔCO ratios are significantly elevated. These proportional values show that the ranges in average values are comparable for DABEX and ACTIVE, at 88% and 98%, respectively, while a higher value of 139% was derived for MILAGRO. The wider variability identified throughout MILAGRO may in part be the result of the longer campaign duration, comprising 23 days of measurements. During this time the site at Paso de Cortes was influenced by air masses of differing origins and is therefore likely to have been subject to emissions from a range of different fire types.

Although there are widespread differences in the average ΔOA/ΔCO identified for different periods throughout each campaign, strong linear relationships are maintained across

aerosol of all ages. The variability within campaigns reflects the potential effects of source conditions and processing in perturbing ΔOA/ΔCO ratios for BB events. However, when all data sets are considered in their entirety, it appears that these effects average out and any differences are compensated, giving a consistent, characteristic ratio for each region. This consistency indicates that while these various factors are capable of propagating localized changes in ΔOA/ΔCO, any such changes are not widespread or uniform enough to create a significant alteration of the overriding ratio established for a given region. The differences in these characteristic ΔOA/ΔCO levels between regions suggest either that a dominant condition or process underpins BB emissions or that potential sources of variability are effectively balanced overall in all locations examined here. The majority of the potential drivers are not characterized extensively enough throughout these campaigns to provide any definitive parametrizations, but they give an indication as to where key uncertainties remain.

3.1. Drivers of Variability. The differences in average ΔOA/ΔCO between separate sampling periods within each campaign are expected to be the manifestation of highly variable properties of individual fire events. However, this analysis shows no evidence for any conclusive relationships with potential drivers, such as geographical influences on fuel types. The maximum (0.520) and minimum (0.238) flight-averaged fresh ΔOA/ΔCO ratios for ACTIVE were actually derived from flights occurring on consecutive days (SD06 and SD07; 23 and 24 November 2005), sampling a fire in a similar location at approximately 12.375° S, 131.592° E. As such, the dominant vegetation and overall range of fuel types contributing to the sampled fire plume are unlikely to have changed significantly given the constrained area, with MODIS Rapid Response hotspot images of the area suggesting that this may indeed have been the same fire or group of fires. It is not possible to provide any further assessment of these effects given the lack of direct observations of source conditions resulting from aircraft measurements, but it would appear that different species typical to a common ecosystem and within a localized environment are potentially capable of producing highly contrasting ERs. Conversely, wider fuel properties such as moisture content, and the implications of these factors for burn conditions, could equally contribute toward the extensive range observed during ACTIVE.

Throughout MILAGRO, there appears to be no correlation between ERs for fresh OA and any specific back trajectory origins (Figure S2, Supporting Information). Although urban emissions are likely to influence the site at Altzomoni given the close proximity to Mexico City,[29] the extent of any effect on overall ΔOA/ΔCO is limited given the much greater magnitude of BB emissions. Several large-scale events in close proximity to the measurement site were observed, most notably between 5 and 6 March, where respective peak ΔOA and ΔCO concentrations exceeded 250 $\mu g \cdot m^{-3}$ and 4000 ppb. In contrast, peak concentrations from urban sources are reported as approximately 60 $\mu g \cdot m^{-3}$ and 550 ppb, respectively, suggesting BB emissions dominate the derived ΔOA/ΔCO ratios. The availability of CO_2 measurements throughout MILAGRO also enabled calculation of modified combustion efficiencies (MCEs), which represent the ratio of excess CO_2 mixing ratios to excess CO_2 and CO combined and give an indication of the dominant combustion phase in associated fires, with MCEs either above or below the threshold of 0.9 indicating a dominance of flaming or smoldering combustion phases, respectively.[7] Changes in combustion conditions are widely purported as one of the main drivers affecting variability in biomass burning emissions.[30,31] However, MCEs calculated for fresh plumes during MILAGRO show no strong correlations with ΔOA/ΔCO beyond the overriding dominance of high MCEs, consistent with the comparatively lower ERs identified throughout the campaign, which are likely to be influenced by reduced total particulate and OA mass fractions from flaming combustion.[3,14]

Although this analysis cannot provide any further clarification of the causes of observed ΔOA/ΔCO variability, the strong regional differences are likely to affect assessments of the global atmospheric aerosol burden. The dominance of OA in PM_1 budgets for these regions implies that the PM_1/ΔCO ratio changes from region to region in response to changing BB emissions. However, if these regional differences prove to be more widespread, then this variability may have significant implications for future BB emission estimates based on remote sensing methods.

3.2. Changes with Age. ΔOA/ΔCO ratios appear to be influenced by the residence time of OA within the atmosphere, in response to levels of physical and chemical processing. ITOP provides the lower extent of the observed range of average ΔOA/ΔCO across the different campaigns included in this analysis, representing the most heavily aged emissions, with measurements taken at the greatest distance from source. The average ratio of 0.019 is equivalent to just 6% of the levels observed during ACTIVE, where both fresh local fire plumes and aged transported air masses were encountered. This lower ratio is likely to be influenced by the long-range transport of air masses sampled during ITOP and the potential for OA removal through precipitation as air is lifted to higher altitudes during convection, along with potential further wet deposition during transportation. Cubison et al.[22] and Hecobian et al.[32] show significantly elevated ΔOA/ΔCO (~0.140) for Canadian boreal forest fires during the Arctic Research of the Composition of the Troposphere from Aircraft and Satellites (ARCTAS) campaign, which involved sampling very close to source. Peltier et al.[33] also identified a lower ΔOA/ΔCO than the values reported by Cubison et al.[22] and Hecobian et al.,[32] reporting ratios from the NEAQS campaign of ~0.050 for the same aged boreal forest fire plumes from Alaska and the Yukon as encountered during ITOP. Despite these consistently lower ΔOA/ΔCO ratios for aged plumes, Petzold et al.[34] suggest there is little evidence for the removal of black carbon (BC) throughout the full duration of transportation, based on the comparison of BC/ΔCO ratios for plumes measured by the DLR Falcon over central Europe with source ERs, although these source profiles are based on the range of EFs reported by Andreae and Merlet[12] rather than specific measurements of Canadian or Alaskan boreal plumes at source. Real et al.[35] also refute the possibility of wet deposition during transportation due to the absence of clouds along the plume path based on European Centre for Medium-range Weather Forecast cloud fields, suggesting that the effect of wet deposition during transportation remains highly uncertain.

Distinguishing between fresh and aged OA in ACTIVE, DABEX, and MILAGRO gives an indication of how processing influences the atmospheric loadings of OA, showing consistently lower ΔOA/ΔCO for the aged fraction in all cases (Figure 1). The greatest relative disparity between fresh and aged fractions was observed during DABEX, where there was a difference of 0.022 between the averages for fresh OA (0.065 ± 0.002) and aged OA (0.043 ± 0.001), equivalent to a change of 34% from the ER near to source. In comparison, smaller differences of 24% and 20%, respectively, were observed during ACTIVE (0.329 ± 0.023 to 0.251 ± 0.005) and MILAGRO (0.051 ± 0.001 to 0.041 ± 0.001).

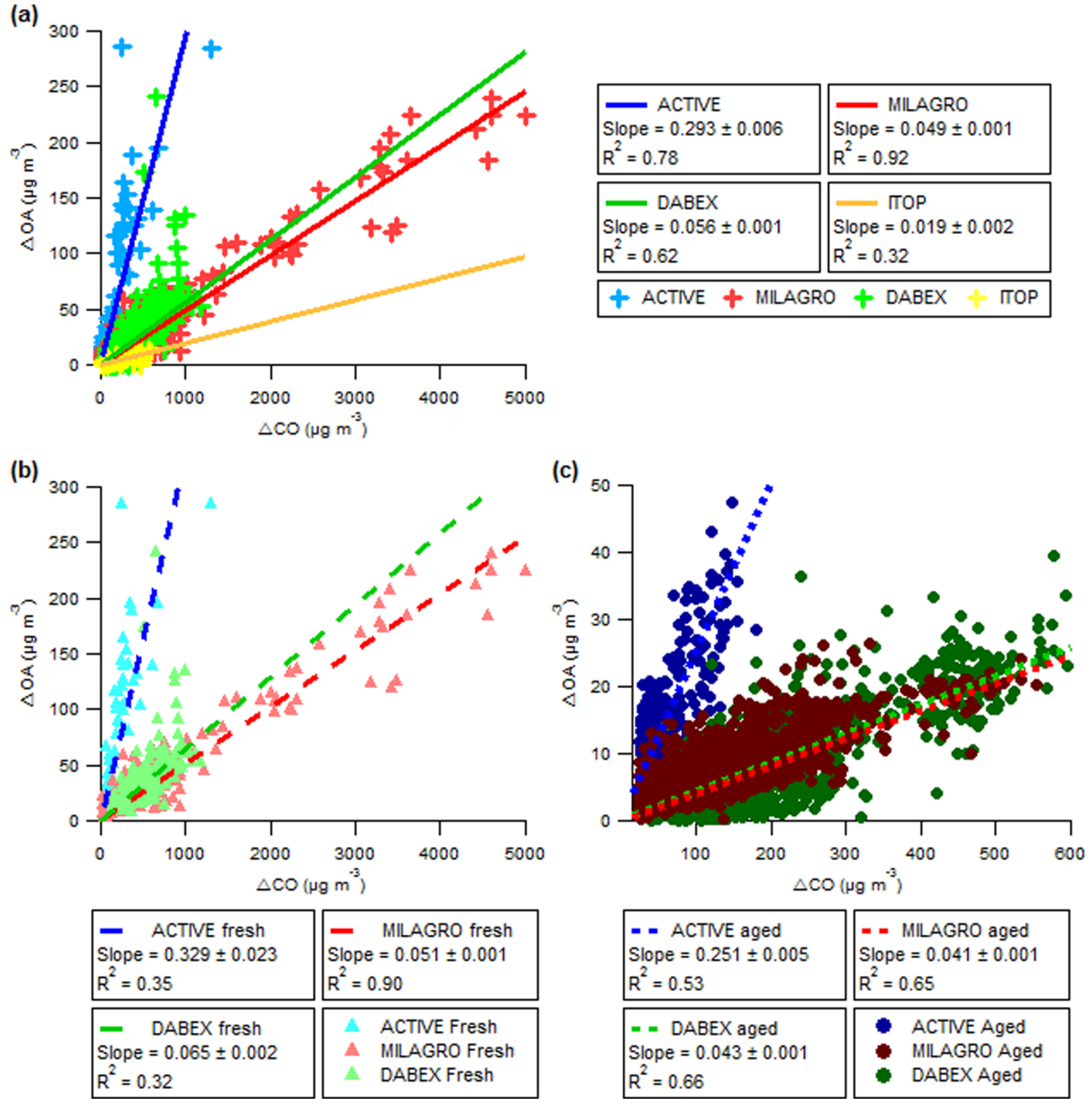

Figure 1. (a) Excess organic aerosol mass concentration versus excess CO for all campaigns. Coefficients are for linear regressions with uncertainties of $\pm 1\sigma$. Average $\Delta OA/\Delta CO$, derived from line slopes, is substantially elevated for ACTIVE above average values from all other campaigns. Fit lines for DABEX and ITOP have been extrapolated using line equations for greater clarity. (b) ΔOA versus ΔCO for segregated fresh and (c) aged OA fractions from ACTIVE, MILAGRO and DABEX. Average $\Delta OA/\Delta CO$ is shown to be consistently higher for fresh OA in comparison to aged OA.

The reduction in $\Delta OA/\Delta CO$ with age throughout DABEX is further substantiated by the concurrent increase in $\Delta O_3/\Delta CO$, where $\Delta O_3/\Delta CO$ is used as a continuous indicator for aging to provide further verification beyond the basic discrete classification of OA as either fresh or aged.

The greater contrast in average $\Delta OA/\Delta CO$ between fresh and aged fractions during DABEX may demonstrate the implications of a changing balance between OA enhancement through secondary formation and OA loss through deposition or physical and chemical transformations during aging, relative to the comparable effects throughout other campaigns. While concentrations of OA and inert marker species such as CO are primarily reduced by dilution as smoke plumes disperse into the ambient atmosphere, OA is also removed through wet deposition and by the evaporation of semivolatile compounds, reducing aerosol concentrations to a greater degree than would be expected from dispersion alone.[36,37] Conversely, the extent to which secondary formation compensates the loss of primary OA may vary, affecting the moderation of $\Delta OA/\Delta CO$ differently between regions. The large contributions of coarse mode aerosol during some DABEX flights provide a potential mechanism for the loss of organic carbon (OC) through preferential secondary condensation to dust particles, reducing the submicrometer OC mass measured by the Q-AMS. Hand et al.[38] provide circumstantial evidence to indicate there may have been condensation of OC onto dust particles, such as the reduced presence of tar balls in mixed dust/biomass burning samples, while Johnson et al.[39] also show an increase in absorption by biomass burning particles downwind from source, indicative of a reduction in highly scattering OC. However, environmental scanning electron microscope analysis showed no discernible differences in particle structure between dust-dominated samples and mixed

Table 2. Mean Values for Composition and Aging Indicators Associated with Segregated Fresh and Aged OA Fractions Throughout Each Campaign[a]

	f_{43}		f_{44}		f_{57}	
	fresh	aged	fresh	aged	fresh	aged
ACTIVE	0.051 ± 0.018	0.057 ± 0.035	0.078 ± 0.043	0.152 ± 0.050	0.011 ± 0.004	0.015 ± 0.012
MILAGRO	0.065 ± 0.006	0.061 ± 0.010	0.099 ± 0.030	0.169 ± 0.028	0.021 ± 0.005	0.013 ± 0.004
DABEX	0.079 ± 0.035	0.104 ± 0.096	0.079 ± 0.030	0.147 ± 0.127	0.023 ± 0.014	0.030 ± 0.054
ITOP		0.109 ± 0.097		0.176 ± 0.137		0.037 ± 0.052
	f_{60}		f_{44}/f_{57}		$\Delta O_3/\Delta CO$	
	fresh	aged	fresh	aged	fresh	aged
ACTIVE	0.006 ± 0.003	0.005 ± 0.003	8.9 ± 7.9	27.4 ± 43.1	0.277 ± 0.147	0.486 ± 0.165
MILAGRO	0.018 ± 0.006	0.006 ± 0.003	5.6 ±3. 7	15.2 ± 7.4	0.382 ± 0.218	0.698 ± 0.201
DABEX	0.011 ± 0.009	0.040 ± 0.072	4.1 ± 2.1	22.3 ± 126.9	0.213 ± 0.052	0.370 ± 0.101
ITOP		0.029 ± 0.049		13.1 ± 16.8		0.837 ± 0.337

[a]With standard deviations of 1σ.

dust/biomass burning particles. As such, the partitioning of processed OC to dust as a potential cause of reduced ΔOA/ΔCO remains highly uncertain. This process is also unlikely to be of significance as a possible fate for SOA throughout either ACTIVE or MILAGRO, where no significant coarse mode was identified.[29,40] Heterogeneous oxidation of OA may also lead to some loss of OA for very long aging times,[41] which may contribute to the lower ΔOA/ΔCO observed for ITOP.

There is little evidence from these data sets to support significant net SOA formation, to the point of a positive impact on ΔOA/ΔCO exceeding other losses. Capes et al.[21] showed that OA became increasingly oxidized with age during DABEX, with an increase in oxygen/carbon ratio (O/C) providing an overall offset for any loss of carbon mass. A stable ΔOA/ΔCO level was therefore maintained, when aerosol of all ages was considered, with a similar result also reported by Cubison et al.[22] for boreal forest fire smoke. However, the shift in the balance of these processes becomes more apparent when older and fresher aerosol are segregated. A number of key OA mass fragments measured by the Q-AMS can be used to infer changes in composition as a result of transformations relating to aging. The m/z 44 fragment is associated with the CO_2^+ ion derived from organic acid species, which form a significant contribution (5−15%) to the overall oxygenated OA mass,[42,43] and is therefore expected to be less prevalent in fresh OA emissions. The ratio of m/z 44 to the total OA concentration (f_{44}) is used as a simplified proxy for the O/C ratio in OA and hence an indicator of aerosol age.[44,45] Although elevated f_{44} levels have been observed in fresh emissions from domestic wood burners,[46] such a trend is not widely apparent for ambient measurements. This is likely to be an effect of the contrasting conditions and behavior of wildfires and controlled burners, with Weimer et al.[46] identifying an increase in f_{44} to dominate the organic mass spectrum for more efficient automatic furnaces where combustion is more complete. Consistency has also been observed between the O/C for laboratory and ambient measurements of open biomass fires, while organic mass (OM)/OC ratios for both are shown to be lower than values for fireplace combustion.[43] Higher mean f_{44} values were observed for the aged OA fraction across all campaigns (Table 2), providing evidence for consistent secondary processing of OA in aging biomass plumes. Mean f_{44}/f_{57} values (where m/z 57 is indicative of fresh primary OA emissions) were also consistently elevated for aged OA compared to fresh OA. However, there are substantial uncertainties associated with the values derived for both age fractions, which must be considered as a major caveat to the identified contrasts in composition. These uncertainties are exacerbated by the reduced signal-to-noise ratio attained by the Q-AMS under aircraft operation, particularly at greater altitudes.[47]

Measurements of both fresh and aged plumes during MILAGRO show a progression toward higher f_{44} and lower f_{60} values with increasing aging (Figure S3, Supporting Information). This trend, characterized by Cubison et al.[21] using measurements from MILAGRO and ARCTAS, alludes to a greater contribution of oxygenated OA and concurrent reduction in primary BB-derived species as plumes age. However, such trends are not observed within measurements from any of the other campaigns included here, most likely as a result of the high levels of noise associated with certain Q-AMS measurements. These issues are particularly evident throughout DABEX and ITOP, where sampling occurred at altitudes of up to 7000 and 10 000 m, respectively, and are also reflected in the large standard deviations quoted in Table 2. The stronger relationships between age and composition apparent throughout MILAGRO are likely to result from an improved signal-to-noise ratio given the longer averaging period applied during data processing.

Hawkins and Russell[10] observed a similar increase in the fraction of oxygenated OA species for progressively more aged emissions from wildfires in California. This increasing level of oxidation, again in the absence of an increase in total OA mass, was attributed to particle phase transformations of OA functional groups as opposed to additional SOA formation. The potential influence of this process on the trends in composition identified throughout this analysis represents a further source of uncertainty regarding the role of SOA formation in BB emissions. As a result, the use of these markers is not able to fully reconcile distributions of ΔOA/ΔCO with the aging processes but gives an indication of the relative influences of OA addition and removal in aging biomass burning plumes, with losses through evaporation, heterogeneous chemistry, and/or deposition persistently matching or exceeding SOA formation.

While there is a consistent reduction in average ΔOA/ΔCO between the fresh and aged OA fractions in all regions, the scales of these changes are always smaller than the associated variability in average fresh ΔOA/ΔCO within each campaign. Throughout ACTIVE, the difference between minimum and maximum flight-averaged values for fresh OA of around 0.28 is

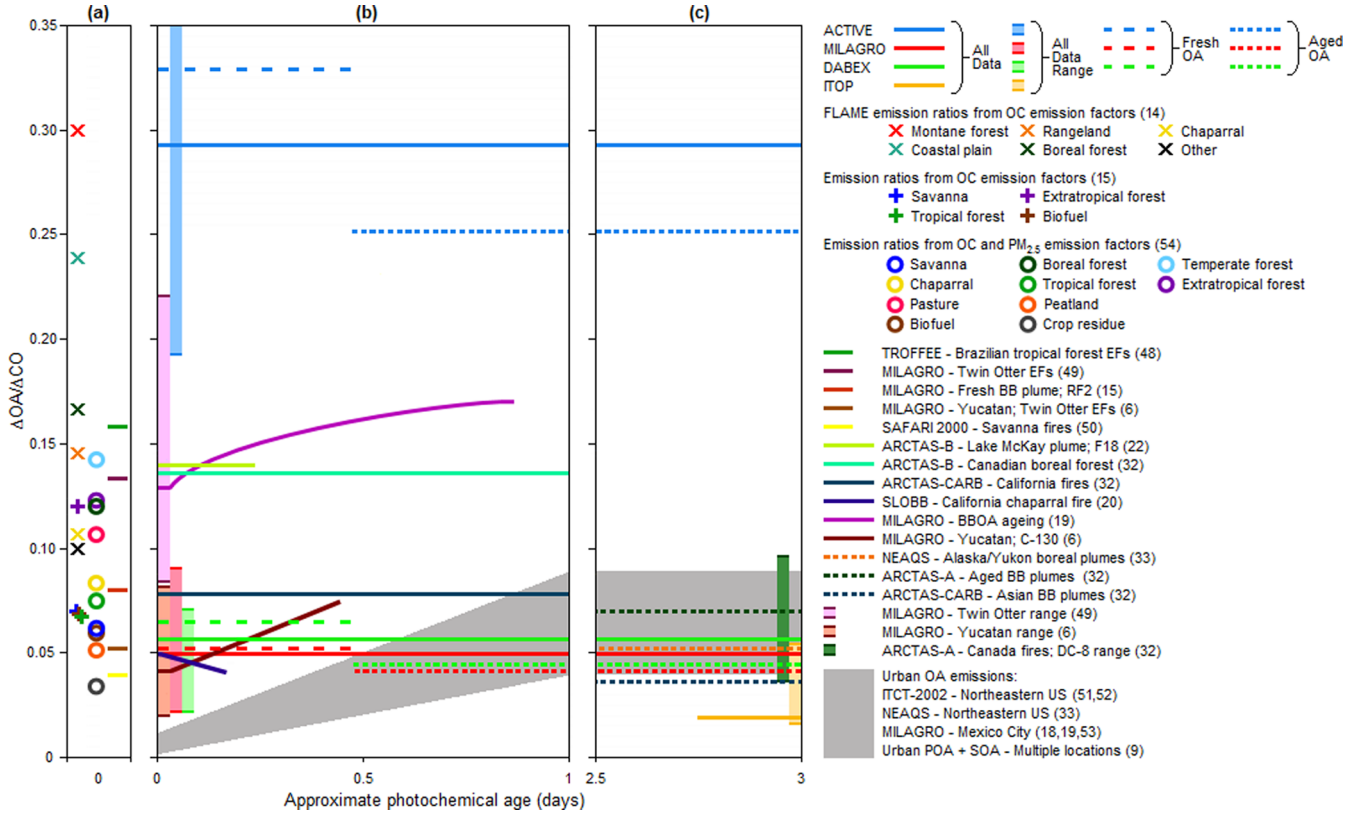

Figure 2. Schematic diagram showing changes in ΔOA/ΔCO with photochemical age in emissions from biomass burning and urban sources. (a) Source emission ratios derived from emission factors calculated during chamber studies[15] or from an ensemble of literature sources.[12,54] (b) Evolution of ΔOA/ΔCO during ~1 day of aging throughout different studies. Tall, narrow bands next to vertical axes show ranges in average ΔOA/ΔCO ratios across separate measurement periods within certain campaigns. (c) Eventual ΔOA/ΔCO after several days aging. *x*-axis values are approximate, given widespread lack of accurate aging constraints. Figure adapted from DeCarlo et al.[19]

nearly 4 times larger than the difference of 0.078 between age fractions, with a similar contrast observed for MILAGRO (0.035 to 0.01). The values from DABEX for flight-to-flight variability (0.028) and change with age (0.022) are more closely comparable, although the variability remains larger. These results emphasize that the effects of BBOA processing appear to be much less significant than initial conditions as a source of uncertainty in emissions. Given the lack of continuous plume sampling throughout these four studies, it is not possible to completely rule out that emissions may have been subject to rapid addition of SOA, as documented by Yokelson et al.[6] Unfortunately, it has not been possible to provide a more rigorous assessment of aerosol composition, or more accurate segregation of POA and SOA, throughout these campaigns. The use of techniques such as positive matrix factorization was not possible for the given data sets due to the insufficient signal-to-noise ratio attainable by the Q-AMS during aircraft deployment. However, with regard to the resolution of regional and global models, the apparent lack of increase in ΔOA/ΔCO for emissions sampled away from source would suggest that any chemical processing is occurring at a subgrid scale. As such, the distinction between POA and combined POA and rapidly formed SOA becomes less significant, as any transformations are occurring on much shorter time scales. Any wider-scale aerosol impacts, such as radiative forcing effects, can be considered to be dominated by what are effectively "primary" emissions with respect to global model resolution. It is therefore increasingly important that consideration of the variability at source is appropriately integrated into model simulations in order to deliver an accurate and appropriate representation of the BBOA fraction.

3.3. Comparisons with BBOA from Other Studies.

Analysis of these four ambient data sets has revealed a number of significant differences in the properties and evolution of BBOA emissions across a range of different environments and atmospheric regimes. Comparison of these results with examples from literature highlights the extent of the variability in average biomass burning ΔOA/ΔCO at source, with a range of more than an order of magnitude across all studies represented here (Figure 2). The large variability in ΔOA/ΔCO between and within the different experiments presented in this study is consistent with the overall variability of ΔOA/ΔCO presented within the literature, as ratios for all four campaigns fall well within the observed spread for biomass burning assessments, including both laboratory and ambient measurements across a range of ages. ACTIVE represents an outlier to the typical range of ΔOA/ΔCO for both fresh and aged fractions, although similarities can be drawn with ERs derived from EFs for controlled burns during the Fire Lab at Missoula Experiment (FLAME; ref 15). The range of EFs reported by McMeeking et al.[15] represents the combustion of plant species that form a significant contribution to the annual wildfire budget in the western and southeastern United States. The highest ER from FLAME was identified for montane forest samples, comprising pine and fir species. Such species are not comparable to the eucalypt forests that dominate the regions studied during ACTIVE (see Supporting Information). However, the coastal plain classification used during FLAME,

comprising myrtle, shrub, and grass species, also produced a similar level of ΔOA/ΔCO as observed during ACTIVE, with potential similarities to vegetation types in areas to the east of Darwin where fires were also sampled. The factor of 3 difference between minimum and maximum ERs is indicative of the high potential variability across different ecosystems and their associated biomass fuels. In contrast, a fairly good level of consistency exists between assessments of boreal forest ERs. Agreement within 40% is observed for all ΔOA/ΔCO ratios close to source in boreal regions, for values taken from both chamber experiments and field campaigns.[22,32,54] Greater divergence is evident among aged ΔOA/ΔCO from boreal fires, although the ratios for heavily aged OA during ITOP increase this spread.

While a net reduction in ΔOA/ΔCO for aged fractions was identified across all projects within this study for which near- and far-field measurements were available, some previous biomass burning studies have shown ΔOA/ΔCO to increase with age close to source in some instances.[6,19] Further evidence exists for the formation of SOA within aging biomass burning plumes across a number of studies, both within the first hour after emission[31] and over a period of several days.[7] Findings from chamber experiments also support substantial SOA formation due to photo-oxidation of wood smoke, with both Grieshop et al.[55] and Hennigan et al.[56] reporting an enhancement in OA mass by up to a factor of 3 over a period of several hours. However, wood burning in closed stoves may be significantly different from open burning, and the dilution conditions in chamber experiments are different from those in the field. These contrasting cases of OA evolution are likely to arise from a shift in the complex balance of various conditions and processes that control OA loss and secondary formation in biomass burning plumes, the full extent of which cannot be elucidated from currently available data sets.

A notable contrast can be identified between biomass burning and urban emission regimes (Figure 2). Numerous studies of anthropogenic urban aerosol emissions consistently show ΔOA/ΔCO to increase with age as a result of SOA formation.[19] These trends with aging have been constrained explicitly where photochemical tracers have been used to determine the age of emissions,[51−53] with further evidence provided by the recurrent increase in ΔOA/ΔCO between POA emissions and combined POA and SOA in urban areas.[9] The absence of similar behavior in biomass burning emissions across a diverse range of locations may be related to the much larger POA emissions of BBOA, at about an order of magnitude larger than urban POA/ΔCO,[9] so that any SOA formation in BB plumes cannot overwhelm the very large POA emissions. As a result, BB emissions may be more susceptible to the greater variability of source conditions. Such differences are evidenced by the observed changes in the nature of ΔOA/ΔCO evolution for BB between regions, in contrast to the greater uniformity identified among urban OA emissions.

The time scales involved in SOA formation, and the stage at which plumes are intercepted, may also affect the ability to observe any increase in ΔOA/ΔCO. During chamber experiments, Grieshop et al.[55] observed a dependence on the VOC/NO_x ratio for OA enhancement in aging wood smoke. The fast rate of OA production identified in that study is consistent with some field observations, which show significant increases in OA mass over periods of less than half a day.[6,19,31] For cases where measurements of aged air masses are performed after a longer period of time, it is possible that any initial increase in ΔOA/ΔCO from SOA formation will have been masked by the aggregate effects of progressive OA loss. In contrast, other studies, including some measuring fresh OA very close to source, show a lack of OA increase over time scales of less than 1 day (refs 20 and 22 and references therein). Given a daytime average atmospheric OH concentration of ∼5 × 10^6 molecules·cm^3, typical in-plume values of (1−1.7) × 10^7 molecules·cm^3 [6,13] represent only around 2−3 times typical concentrations. Therefore, these changes are not likely to cause aging to occur on such a rapid time scale that it cannot be observed through aircraft measurements. With the exception of ITOP, where only highly aged plumes were encountered, each campaign included measurements of active fires very close to source and within a time scale of less than 1 hour since emission (see Supporting Information). Conversely to the possibility of unobserved, very rapid SOA formation, the absence of any sustained increase in ΔOA/ΔCO with aging throughout these regions may be a result of greater losses of POA through evaporation of more volatile aerosol, to such an extent that the addition of SOA simply maintains ΔOA/ΔCO at a stable level rather than presenting any identifiable enhancement. The causes of these observed discrepancies between studies therefore remain unclear, with a range of different factors potentially affecting the apparent evolution of ΔOA/ΔCO with aging. However, the regional differences in biomass burning ΔOA/ΔCO ratios, together with the inherent chaotic and unpredictable nature of biomass fires driving variability near to source, underlie the variability in the atmospheric burden of BBOA. As such, these uncertainties are likely to contribute toward reported discrepancies between measurements and model estimates,[57] restricting reliable global-scale prediction of biomass burning aerosol loadings and their climate effects. Improved parametrization of BBOA in global models is therefore dependent on continued advances in the characterization of aerosol properties and their evolution to understand the causes and implications of this variability, through integration of laboratory measurements and field studies.

■ ASSOCIATED CONTENT

Ⓢ Supporting Information

Additional text, describing campaign backgrounds, instrumentation, fire types and plume ages, and MILAGRO back trajectories and ΔOA/ΔCO variability; and three figures, showing ΔOA and ΔCO time series for all campaigns; a satellite image of the region surrounding the MILAGRO study site, detailing back trajectories throughout the measurement period; and ΔOA vs ΔCO plots for fresh and aged OA fractions with color scales denoting various compositional parameters. This material is available free of charge via the Internet at http://pubs.acs.org/.

■ AUTHOR INFORMATION

Corresponding Author

*E-mail: matthew.jolleys@postgrad.manchester.ac.uk.

Notes

The authors declare no competing financial interest.

■ ACKNOWLEDGMENTS

We acknowledge financial support from the United Kingdom Natural Environment Research Council (NERC). NERC provided funding for several of the projects included in this study, including ACTIVE (NE/C512688/1), ITOP (NER/T/S/2002/00579), and DABEX-DODO, as part of AMMA-UK (NE/B505562/1 and NE/C517292/1). The deployment of the Q-AMS at Paso de Cortez during MILAGRO was funded by NSF (ATM 05-11772)

and DOE (W/GEC05-010 and MPC35TA-A5) grants, with participation supported by the Royal Society International Joint Projects scheme. Additional thanks goes to the NERC Airborne Research and Survey Facility (ASRF) for operational support of the Dornier-228 aircraft, and the Facility for Airborne Atmospheric Measurements (FAAM), together with DirectFlight, Avalon, the Met Office and the BAe-146 air and ground crews. M.D.J. was supported by a NERC studentship NE/H525162/1. J.L.J. was supported by DOE (BER, ASR) DE-SC0006035 and DE-FG02-11ER65293 and NASA NNX12AC03G.

REFERENCES

(1) Bond, T. C. A technology-based global inventory of black and organic carbon emissions from combustion. *J. Geophys. Res., [Atmos.]* **2004**, *109*, No. D14203.
(2) Hobbs, P. V.; et al. Direct radiative forcing by smoke from biomass burning. *Science* **1997**, *275* (5307), 1776−1778.
(3) Reid, J. S.; et al. A review of biomass burning emissions part II: Intensive physical properties of biomass burning particles. *Atmos. Chem. Phys.* **2005**, *5*, 799−825.
(4) Asa-Awuku, A.; et al. Investigation of molar volume and surfactant characteristics of water-soluble organic compounds in biomass burning aerosol. *Atmos. Chem. Phys.* **2008**, *8* (4), 799−812.
(5) Penner, J. E., et al. Aerosols, their direct and indirect effects. In *Climate Change 2001: The Scientific Basis. Contribution of Working Group I to the Third Assessment Report of the Intergovernmental Panel on Climate Change*; Houghton, J. T., et al., Eds.; Cambridge University Press: Cambridge, U.K., and New York, 2001; pp 289−348.
(6) Yokelson, R. J.; et al. Emissions from biomass burning in the Yucatan. *Atmos. Chem. Phys.* **2009**, *9* (15), 5785−5812.
(7) Reid, J. S.; et al. Physical, chemical, and optical properties of regional hazes dominated by smoke in Brazil. *J. Geophys. Res., [Atmos.]* **1998**, *103* (D24), 32059−32080.
(8) Abel, S. J.; et al., Evolution of biomass burning aerosol properties from an agricultural fire in southern Africa. *Geophys. Res. Lett.* **2003**, *30*, (15).
(9) De Gouw, J.; Jimenez, J. L. Organic aerosols in the Earth's atmosphere. *Environ. Sci. Technol.* **2009**, *43* (20), 7614−7618.
(10) Hawkins, L. N.; Russell, L. M. Oxidation of ketone groups in transported biomass burning aerosol from the 2008 Northern California Lightning Series fires. *Atmos. Environ.* **2010**, *44* (34), 4142−4154.
(11) LeCanut, P.; et al. Airborne studies of emissions from savanna fires in southern Africa. 1. Aerosol emissions measured with a laser optical particle counter. *J. Geophys. Res., [Atmos.]* **1996**, *101* (D19), 23615−23630.
(12) Andreae, M. O.; Merlet, P. Emission of trace gases and aerosols from biomass burning. *Glob. Biogeochem. Cycles* **2001**, *15* (4), 955−966.
(13) Hobbs, P. V.; et al. Evolution of gases and particles from a savanna fire in South Africa. *J. Geophys. Res.* **2003**, *108* (D13), 8485.
(14) Ferek, R. J.; et al. Emission factors of hydrocarbons, halocarbons, trace gases and particles from biomass burning in Brazil. *J. Geophys. Res., [Atmos.]* **1998**, *103* (D24), 32107−32118.
(15) McMeeking, G. R. Emissions of trace gases and aerosols during the open combustion of biomass in the laboratory. *J. Geophys. Res., [Atmos.]* **2009**, *114*, No. D19210.
(16) Volkamer, R. Secondary organic aerosol formation from anthropogenic air pollution: Rapid and higher than expected. *Geophys. Res. Lett.* **2006**, *33*, No. L17811.
(17) Zhang, Q.; et al. Understanding atmospheric organic aerosols via factor analysis of aerosol mass spectrometry: a review. *Anal. Bioanal. Chem.* **2011**, *401* (10), 3045−3067.
(18) DeCarlo, P. F.; et al. Fast airborne aerosol size and chemistry measurements above Mexico City and Central Mexico during the MILAGRO campaign. *Atmos. Chem. Phys.* **2008**, *8* (14), 4027−4048.
(19) DeCarlo, P. F.; et al. Investigation of the sources and processing of organic aerosol over the Central Mexican Plateau from aircraft measurements during MILAGRO. *Atmos. Chem. Phys.* **2010**, *10* (12), 5257−5280.
(20) Akagi, S. K.; et al. Evolution of trace gases and particles emitted by a chaparral fire in California. *Atmos. Chem. Phys.* **2012**, *12* (3), 1397−1421.
(21) Capes, G. Aging of biomass burning aerosols over West Africa: Aircraft measurements of chemical composition, microphysical properties, and emission ratios. *J. Geophys. Res., [Atmos.]* **2008**, *113*, No. D00C15.
(22) Cubison, M. J.; et al. Effects of aging on organic aerosol from open biomass burning smoke in aircraft and laboratory studies. *Atmos. Chem. Phys.* **2011**, *11* (23), 12049−12064.
(23) Schneider, J.; et al. Mass spectrometric analysis and aerodynamic properties of various types of combustion-related aerosol particles. *Int. J. Mass Spectrom.* **2006**, *258* (1−3), 37−49.
(24) Alfarra, M. R.; et al. Identification of the mass spectral signature of organic aerosols from wood burning emissions. *Environ. Sci. Technol.* **2007**, *41* (16), 5770−5777.
(25) Aiken, A. C.; et al. Mexico City aerosol analysis during MILAGRO using high resolution aerosol mass spectrometry at the urban supersite (T0) - Part 1: Fine particle composition and organic source apportionment. *Atmos. Chem. Phys.* **2009**, *9* (17), 6633−6653.
(26) Andreae, M. O.; Rosenfeld, D. Aerosol-cloud-precipitation interactions. Part 1. The nature and sources of cloud-active aerosols. *Earth-Sci. Rev.* **2008**, *89* (1−2), 13−41.
(27) Mason, S. A.; et al. Complex effects arising in smoke plume simulations due to inclusion of direct emissions of oxygenated organic species from biomass combustion. *J. Geophys. Res., [Atmos.]* **2001**, *106* (D12), 12527−12539.
(28) Herndon, S. C. Correlation of secondary organic aerosol with odd oxygen in Mexico City. *Geophys. Res. Lett.* **2008**, *35*, No. L15804.
(29) Baumgardner, D.; et al. Physical and chemical properties of the regional mixed layer of Mexico's Megapolis. *Atmos. Chem. Phys.* **2009**, *9* (15), 5711−5727.
(30) Yokelson, R. J.; et al. Trace gas and particle emissions from open biomass burning in Mexico. *Atmos. Chem. Phys.* **2011**, *11* (14), 6787−6808.
(31) Gao, S. Water-soluble organic components in aerosols associated with savanna fires in southern Africa: Identification, evolution, and distribution. *J. Geophys. Res., [Atmos.]* **2003**, *108* (D13), 8941.
(32) Hecobian, A.; et al. Comparison of chemical characteristics of 495 biomass burning plumes intercepted by the NASA DC-8 aircraft during the ARCTAS/CARB-2008 field campaign. *Atmos. Chem. Phys.* **2011**, *11* (24), 13325−13337.
(33) Peltier, R. E.; et al. Fine aerosol bulk composition measured on WP-3D research aircraft in vicinity of the Northeastern United States - results from NEAQS. *Atmos. Chem. Phys.* **2007**, *7* (12), 3231−3247.
(34) Petzold, A.; et al. Perturbation of the European free troposphere aerosol by North American forest fire plumes during the ICARTT-ITOP experiment in summer 2004. *Atmos. Chem. Phys.* **2007**, *7* (19), 5105−5127.
(35) Real, E. Processes influencing ozone levels in Alaskan forest fire plumes during long-range transport over the North Atlantic. *J. Geophys. Res., [Atmos.]* **2007**, *112*, No. D10S41.
(36) Robinson, A. L.; et al. Rethinking organic aerosols: Semivolatile emissions and photochemical aging. *Science* **2007**, *315* (5816), 1259−1262.
(37) Shrivastava, M. K.; et al. Modeling semivolatile organic aerosol mass emissions from combustion systems. *Environ. Sci. Technol.* **2006**, *40* (8), 2671−2677.
(38) Hand, V. L. Evidence of internal mixing of African dust and biomass burning particles by individual particle analysis using electron beam techniques. *J. Geophys. Res., [Atmos.]* **2010**, *115*, No. D13301.
(39) Johnson, B. T. Aircraft measurements of biomass burning aerosol over West Africa during DABEX. *J. Geophys. Res., [Atmos.]* **2008**, *113*, No. D00C06.

(40) Allen, G. Aerosol and trace-gas measurements in the Darwin area during the wet season. *J. Geophys. Res., [tmos.* **2008**, *113*, No. D06306.
(41) George, I. J. Chemical aging of ambient organic aerosol from heterogeneous reaction with hydroxyl radicals. *Geophys. Res. Lett.* **2008**, *35*, No. L13811.
(42) Alfarra, M. R.; et al. Characterization of urban and rural organic particulate in the lower Fraser valley using two aerodyne aerosol mass spectrometers. *Atmos. Environ.* **2004**, *38* (34), 5745−5758.
(43) Aiken, A. C.; et al. O/C and OM/OC ratios of primary, secondary, and ambient organic aerosols with high-resolution time-of-flight aerosol mass spectrometry. *Environ. Sci. Technol.* **2008**, *42* (12), 4478−4485.
(44) Ng, N. L.; et al. Changes in organic aerosol composition with aging inferred from aerosol mass spectra. *Atmos. Chem. Phys.* **2011**, *11* (13), 6465−6474.
(45) Morgan, W. T.; et al. Airborne measurements of the spatial distribution of aerosol chemical composition across Europe and evolution of the organic fraction. *Atmos. Chem. Phys.* **2010**, *10* (8), 4065−4083.
(46) Weimer, S. Organic aerosol mass spectral signatures from wood-burning emissions: Influence of burning conditions and wood type. *J. Geophys. Res., [Atmos.]* **2008**, *113*, No. D10304.
(47) Morgan, W. T.; et al. Vertical distribution of sub-micron aerosol chemical composition from North-Western Europe and the North-East Atlantic. *Atmos. Chem. Phys.* **2009**, *9* (15), 5389−5401.
(48) Yokelson, R. J.; et al. The Tropical Forest and Fire Emissions Experiment: overview and airborne fire emission factor measurements. *Atmos. Chem. Phys.* **2007**, *7* (19), 5175−5196.
(49) Yokelson, R. J.; et al. Emissions from forest fires near Mexico City. *Atmos. Chem. Phys.* **2007**, *7* (21), 5569−5584.
(50) Sinha, P.; et al. Emissions of trace gases and particles from savanna fires in southern Africa. *J. Geophys. Res., [Atmos.]* **2003**, *108* (D13), 8487.
(51) de Gouw, J. A. Budget of organic carbon in a polluted atmosphere: Results from the New England Air Quality Study in 2002. *J. Geophys. Res., [Atmos.]* **2005**, *110*, No. D16305.
(52) Kleinman, L. I. Aircraft observations of aerosol composition and ageing in New England and Mid-Atlantic States during the summer 2002 New England Air Quality Study field campaign. *J. Geophys. Res., [Atmos.]* **2007**, *112*, No. D09310.
(53) Dzepina, K.; et al. Evaluation of recently-proposed secondary organic aerosol models for a case study in Mexico City. *Atmos. Chem. Phys.* **2009**, *9* (15), 5681−5709.
(54) Akagi, S. K.; et al. Emission factors for open and domestic biomass burning for use in atmospheric models. *Atmos. Chem. Phys.* **2011**, *11* (9), 4039−4072.
(55) Grieshop, A. P.; et al. Laboratory investigation of photochemical oxidation of organic aerosol from wood fires 1: measurement and simulation of organic aerosol evolution. *Atmos. Chem. Phys.* **2009**, *9* (4), 1263−1277.
(56) Hennigan, C. J.; et al. Chemical and physical transformations of organic aerosol from the photo-oxidation of open biomass burning emissions in an environmental chamber. *Atmos. Chem. Phys.* **2011**, *11* (15), 7669−7686.
(57) Kaiser, J. W.; et al. Biomass burning emissions estimated with a global fire assimilation system based on observed fire radiative power. *Biogeosciences* **2012**, *9*, 527−554.

Characterizing the aging of biomass burning organic aerosol using mixing ratios – a meta-analysis of four regions

Matthew D. Jolleys[*1], Hugh Coe[1], Gordon McFiggans[1], Gerard Capes[1], James D. Allan[1,2], Jonathan Crosier[1,2], Paul I. Williams[1,2], Grant Allen[1], Keith N. Bower[1], Jose L. Jimenez[3], Lynn M. Russell[4], Michel Grutter[5], Darrel Baumgardner[5]*

* Corresponding author email: matthew.jolleys@postgrad.manchester.ac.uk

[1] Centre for Atmospheric Science, School of Earth, Atmospheric and Environmental Science, University of Manchester, UK

[2] National Centre for Atmospheric Science, University of Manchester, UK

[3] Cooperative Institute of Research in the Environmental Sciences and Department of Chemistry and Biochemistry, University of Colorado, Boulder, Colorado, USA

[4] Scripps Institution of Oceanography, University of California San Diego, La Jolla, California, USA

[5] Centro de Ciencias de la Atmósfera, Universidad Nacional Autónoma de México, Mexico City, Mexico

Supplementary material for the manuscript submitted to Environmental Science & Technology

Contents:

15 pages

Text ST1 – ST4

3 figures

References

ST1. Campaign backgrounds

The ACTIVE experiment was carried out between November 2005 and February 2006 around the Darwin region of northern Australia (*S1, S2*). Measurements of BBOA were most widespread during the 2005 part of the campaign, coinciding with the biomass burning season within the region, prior to the onset of the monsoon period. Biomass burning influences within the region included both local fires and more aged, transported emissions from fires to the east in Queensland. All data considered here were obtained from flights performed by the NERC Dornier-228 aircraft, covering the local Darwin area and the Tiwi Islands to the north, where several active fires were surveyed.

DABEX and DODO (Dust Outflow and Deposition to the Ocean, hereafter referred to singularly as DABEX) formed part of the wider AMMA (African Monsoon Multidisciplinary Analyses) program, with the FAAM BAe-146 aircraft deployed in a series of flights across West Africa throughout February 2006 (*S3, S4*). DABEX flights originated from Niamey in Niger, and targeted fresh biomass burning emissions from widespread fires to the south over Benin and Nigeria, along with more aged emissions at higher altitudes. Layers of lofted aged biomass burning aerosol were also encountered during DODO flights, flying from Dakar in Senegal, further to the west and downwind from the region surveyed throughout DABEX.

The final aircraft dataset included in this analysis came from further FAAM flights during the ITOP campaign in July and August 2004 (*S5*), as part of the International Consortium for Atmospheric Research on Transport and Transformation (ICARTT; *S6*). The wider scope of ICARTT included measurements of emissions from boreal forest fires in North America. Highly aged plumes from these fires were sampled by the BAe-146 around the Azores, following advection across the North Atlantic. Data selection throughout ITOP followed the direction of Lewis et al. (*S5*), where biomass burning influences were inferred from back trajectory cluster analysis, showing repeated transport from Alaska and Northern Canada.

A further ground-based dataset was acquired from a site at Altzomoni (19.117° N, 98.654° W), located near the Paso de Cortez to the southeast of Mexico City (*S7*). Continuous measurements were performed throughout the duration of March 2006, in parallel with the broader MILAGRO series of atmospheric measurements (*S8*), which involved a number of intensive studies at ground-based supersites within the Mexico City Metropolitan Area (MCMA). While the main objectives of MILAGRO focused on the assessment of anthropogenic emissions from the MCMA, the site at Altzomoni was strongly influenced by biomass burning, with contributions from both local mountain forest fires and savanna fires to the southeast of the city region (*S9*).

ST2. Instrumentation

The Q-AMS provides high time resolution (30 seconds), size-resolved measurement of sub-micron aerosol mass and composition (*S10*). Concentrations of all major non-refractory aerosol species are retrieved from sampled mass spectra, for *m/z* ratios from 0 to 300 at unit mass resolution. Peaks associated with certain ions can therefore be related to specific organic components, and used to infer the component contributions to the overall OA mass. Total particle number concentrations were measured with TSI Inc. condensation particle counters (CPCs) in each campaign, with a model 3010 CPC used during ACTIVE and MILAGRO, and a model 3025 Ultrafine CPC for all flights on the BAe-146. In each instance, concentrations of gaseous species and aerosol number concentrations, along with positional data, were averaged to the Q-AMS timebase, given the lower temporal resolution of the Q-AMS relative to the other instruments used (typically 1 second).

Accuracy of Q-AMS measurements under laboratory conditions were evaluated by Drewnick et al. (*S11*), with a reported minimum detection limit for the organic fraction of 0.5 μg m^{-3}. Crosier et al. (*S12*) observed a detection limit of 1.69 ug m^{-3} for 30-second aircraft

measurements of OA at an altitude of 1000 m. However, this figure is expected to increase with altitude, as indicated by airborne measurements of vertical aerosol distribution in northern Europe, which show an increasing variability about the mean OA concentration by around a factor of 11 for 500m altitude bins between 500 m and 11 km (*S13*). The precision of Q-AMS measurements in response to instrument noise was estimated to be approximately 3.3 ug m^{-3} by Capes et al. (*S14*) for 30-second aircraft measurements at an altitude of 600 m.

All Q-AMS measurements were corrected for collection efficiency (CE) as part of the initial data processing. Allen et al. (*S1*) report ratios of between 0.4 and 0.7 for the comparison of UHSAS particulate volume to accumulated AMS and PSAP volume during ACTIVE, resulting in a derived CE of 0.5. Baumgardner et al. (*S7*) demonstrated the closure between AMS and BC mass and volume derived from SMPS size distributions for MILAGRO. A lower CE of 0.34 was calculated by Capes et al. (*S3*) for DABEX, indicating that the AMS may provide a lower measure of mass compared to estimates derived from PCASP size distributions given the contributions of BC and mineral dust within the study region. A collection efficiency of 0.5 was also calculated for ITOP through comparison of AMS data with measurements of aerosol composition by PILS-IC.

ST3. Fire types and plume ages

Given the predominance of aircraft measurements throughout these campaigns, it has not been widely possible to obtain accurate classifications of fires within each region. Similarly, the lack of an extensive range of photochemical measurements limits the ability to accurately constrain plume ages. However, these details can be inferred to an extent from wider sources, in order to provide an overview of the nature of sampled emissions. Detailed vegetation maps covering the regions subject to widespread fires during ACTIVE are available from the Territory Natural Resource Management/Charles Darwin University

Cooperative Research Centre for Tropical Savannas Management's Northern Land Manager service (*S15*-*S18*). These maps indicate that the region surveyed during ACTIVE was generally dominated by eucalypt forests and woodlands, characterized by the species *Eucalyptus tetrodonta* and *Eucalyptus miniata*. The Tiwi Islands also contain smaller pockets of acacia shrubland and mangrove swamps, while the region immediately to the east of Darwin where several active fires were also sampled features areas of grassland, wetland and tea tree swamps. During the ACTIVE study period large scale land clearance was taking place across both Arnhem Land and the Cape York Peninsula in northern Queensland, as evidenced by MODIS fire maps (*S1*). Arnhem Land consists of fairly extensive heathlands and areas of tea tree woodlands and wetlands, with tea tree woodlands also widespread along the eastern and western fringes of Cape York, along with areas of wet heath, grassland and rainforest. Observations of active fires indicate that some plumes were sampled directly at source, while aged emissions from fires in Arnhem Land and Cape York were transported over a period of up to five days (*S1*).

Measurements of BB plumes during DABEX took place at a wide range of distances from source. Johnson et al. (*S19*) report sampling active fires at a height of 300 m, while layers of more aged emissions and regional hazes were encountered downwind from the source region, up to several days after emission. Small agricultural fires were widespread across the region throughout the duration of the campaign, with grasses, scrub vegetation and agricultural residues expected to constitute the dominant fuel types. Observations indicate that both flaming and smoldering combustion phases were occurring throughout these fires. Grass fires were also prevalent during MILAGRO, while many small shrub and agricultural fires were observed across the wider Mexico City region (*S20*). Back trajectory analysis suggests aged emissions had been transported for between three and five days prior to measurement, as inferred from the locations of potential BB source regions beyond the local area.

Aged plumes sampled during ITOP were also encountered at other positions across their transit as part of further aircraft studies within the wider ICARTT program. Both the NASA DC8 and the DLR Falcon performed measurements of the plumes, over Newfoundland and continental Europe respectively. Using a combination of these observations and back trajectory simulations, Real et al. (*S21*) and Petzold et al. (*S22*) suggest that the plumes had been transported for between three and six days before being sampled around the Azores. Furthermore, model simulations of plume evolution have shown high levels of photochemical activity, with strong O_3 production during transportation towards Europe. Mixing and dilution of plumes with surrounding air also appears to have a significant effect, as indicated by the large observed decrease in CO concentrations with increasing distance from source (*S21*).

ST4. MILAGRO back trajectories and ΔOA/ΔCO variability

Daily distributions of individual fresh ΔOA/ΔCO values throughout MILAGRO appear to be characterised by two distinct modes. Between the 5th and 9th March, the peak frequency occurs between 0.03 and 0.07, followed by a rapid decrease in frequency above this threshold. Between the 10th and 17th March there is a pronounced change in ΔOA/ΔCO distribution, as peaks tend to occur at a higher position and frequencies do not decrease as consistently above 0.07. Distributions are most substantially shifted towards higher values on the 10th, 15th and 17th, with ΔOA/ΔCO greater than 0.1 for 31%, 46% and 77% of datapoints on each of these dates respectively. There is also no consistent relationship between the two ΔOA/ΔCO modes and back trajectory origins. Between the 15th and 17th March, when the most significant enhancements in ΔOA/ΔCO distribution were identified, with more than 60% of values above 0.07 on each day, sampled air masses had originated from the northeast and north five days prior to detection at the measurement site, switching to an easterly

approach in the final 24 hours before arrival. A comparable change in ΔOA/ΔCO was observed on the 10th and 12th, when back trajectories indicated a shift in origin to the west and southwest. Although this back trajectory pattern was also identified on the 9th and 11th, ΔOA/ΔCO distributions for these dates show better agreement with the low ΔOA/ΔCO mode observed earlier in the month. ΔOA/ΔCO values from the 23rd also conform to this initial trend, again peaking between 0.04 and 0.06, despite a further change in back trajectories towards the northwest.

The elevated ΔOA/ΔCO distributions identified on the 12th and 15th-17th March coincided with an enhancement in the $\Delta O_3/\Delta CO$ distribution, suggesting an increase in photochemical processing within these plumes and possible influence by SOA formation. However, there is no such shift in $\Delta O_3/\Delta CO$ distribution on the 10th March, when ΔOA/ΔCO was also higher. Furthermore, these trends show poor consistency with aerosol composition. While f_{44} and f_{57} distributions generally show reconciliatory correlations with ΔOA/ΔCO for the days on which the latter is increased, these trends are also repeated on days when ΔOA/ΔCO is low. These discrepancies highlight the limitations in attributing more finite ΔOA/ΔCO variability to compositional changes.

Figure S1: ΔOA and ΔCO time series for (a) ACTIVE, (b) MILAGRO, (c) DABEX and (d) ITOP. Data is shown for all flights or dates where sufficient data were available to contribute to overall campaign datasets following screening by f_{60}, ΔCO and number concentration thresholds. Grey sections represent data removed by screening and subsequently omitted from analysis.

Figure S2: MODIS satellite image of central Mexico, showing one and five day back trajectories from Altzomoni (19.117° N, 98.654° W) initiated at 650 mb at 1800 UTC (1200 local time), as provided by the BADC Web Trajectory service (http://badc.nerc.ac.uk/community/trajectory/). Back trajectories are shown for all days on which fresh OA plumes were identified. *Inset:* (a) ΔOA/ΔCO and (b) $\Delta O_3/\Delta CO$ distributions for fresh OA during MILAGRO. Grey sections show percentage values averaged across corresponding bins for each day, while black sections represent the distribution of counts as a percentage of total counts.

Figure S3: ΔOA vs. ΔCO plots for (a) ACTIVE, (b) MILAGRO, (c) DABEX and (d) ITOP, segregated into (i) fresh and (ii) aged OA fractions, coloured by (left to right) f_{44}/f_{57}, f_{44}, f_{57} and f_{60} respectively. Distinctions in the composition of BBOA between age fractions are most evident during MILAGRO. Several moderate trends can also be identified within the aged OA fraction for MILAGRO which consistently indicate a decrease in OA/ΔCO with progressive ageing. Both f_{44}/f_{57} and f_{44}, as indicators for ageing, are generally negatively correlated with OA/ΔCO. In contrast, f_{57} and f_{60}, which represent the proportional abundances of characteristic fresh OA components, show overall positive trends with ΔOA/ΔCO. Evidence for similar relationships within the fresh OA fraction is limited.

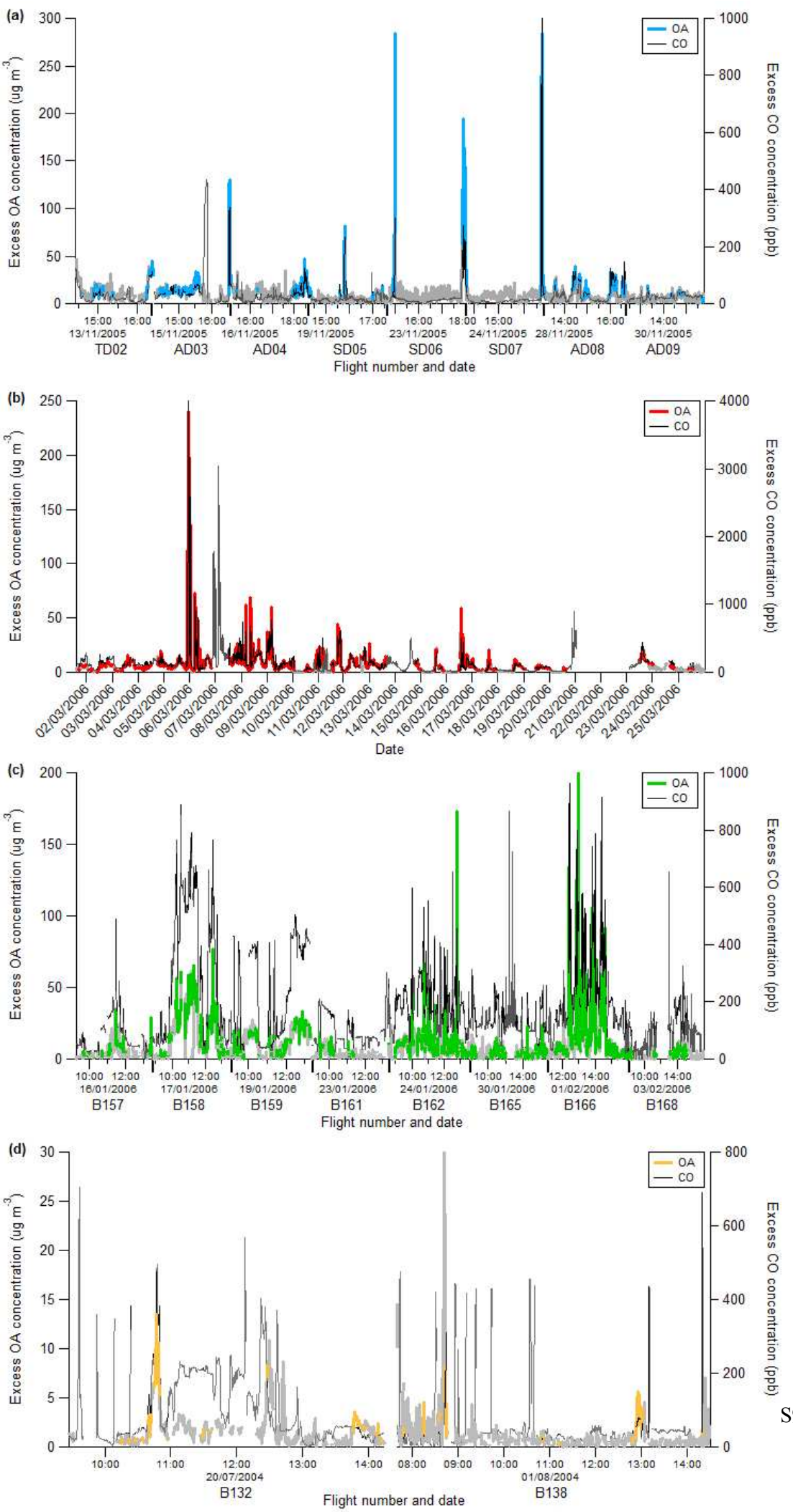
(a)
Excess OA concentration (ug m-3)
Excess CO concentration (ppb)
OA
CO
15:00 13/11/2005
16:00
15:00 15/11/2005
16:00
16:00 16/11/2005
18:00
15:00 19/11/2005
17:00
16:00 23/11/2005
18:00
15:00 24/11/2005
14:00 28/11/2005
16:00
14:00 30/11/2005
TD02
AD03
AD04
SD05
SD06
SD07
AD08
AD09
Flight number and date
(b)
Excess OA concentration (ug m-3)
Excess CO concentration (ppb)
OA
CO
02/03/2006
03/03/2006
04/03/2006
05/03/2006
06/03/2006
07/03/2006
08/03/2006
09/03/2006
10/03/2006
11/03/2006
12/03/2006
13/03/2006
14/03/2006
15/03/2006
16/03/2006
17/03/2006
18/03/2006
19/03/2006
20/03/2006
21/03/2006
22/03/2006
23/03/2006
24/03/2006
25/03/2006
Date
(c)
Excess OA concentration (ug m-3)
Excess CO concentration (ppb)
OA
CO
10:00 12:00 16/01/2006
B157
10:00 12:00 17/01/2006
B158
10:00 12:00 19/01/2006
B159
10:00 12:00 23/01/2006
B161
10:00 12:00 24/01/2006
B162
10:00 14:00 30/01/2006
B165
12:00 14:00 01/02/2006
B166
10:00 14:00 03/02/2006
B168
Flight number and date
(d)
Excess OA concentration (ug m-3)
Excess CO concentration (ppb)
OA
CO
10:00 11:00 12:00 13:00 14:00 20/07/2004
B132
08:00 09:00 10:00 11:00 12:00 13:00 14:00 01/08/2004
B138
Flight number and date

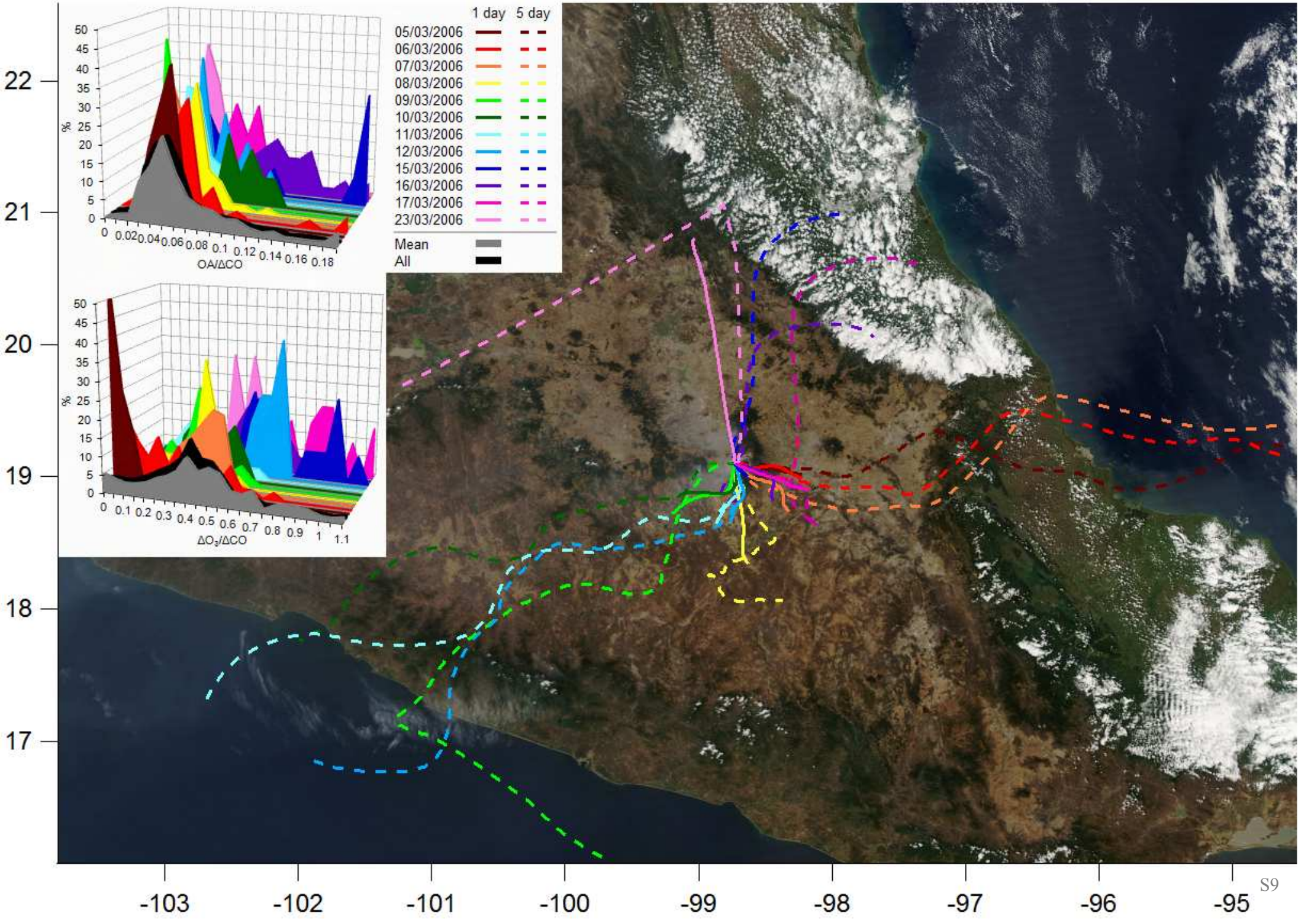
1 day
5 day
05/03/2006
06/03/2006
07/03/2006
08/03/2006
09/03/2006
10/03/2006
11/03/2006
12/03/2006
15/03/2006
16/03/2006
17/03/2006
23/03/2006
Mean
All
%
OA/ΔCO
ΔO3/ΔCO
22
21
20
19
18
17
-103
-102
-101
-100
-99
-98
-97
-96
-95

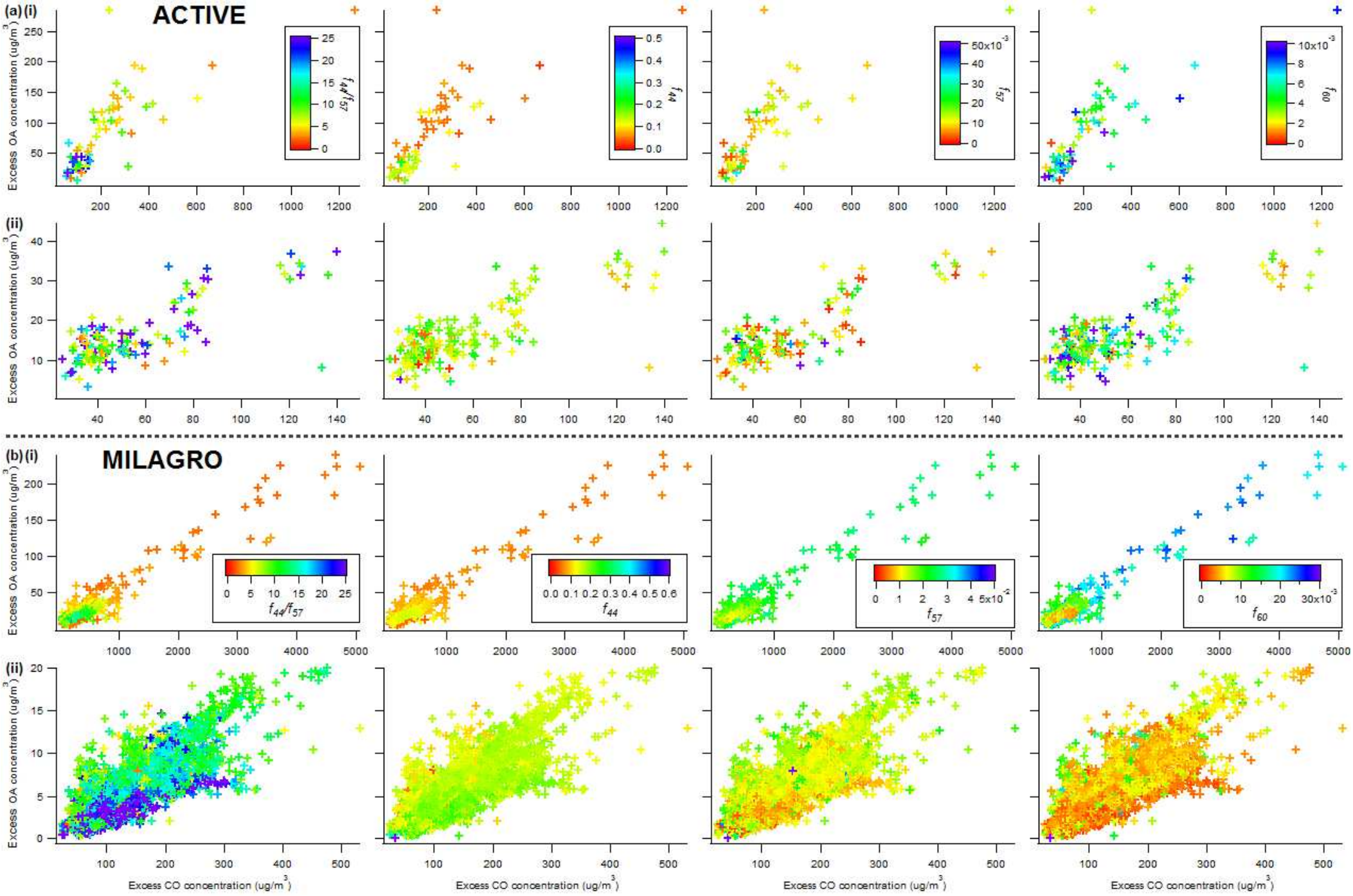
(a) (i)
ACTIVE
(ii)
(b) (i)
MILAGRO
(ii)
Excess OA concentration (ug/m3)
Excess CO concentration (ug/m3)
f44/f57
f44
f57
f60

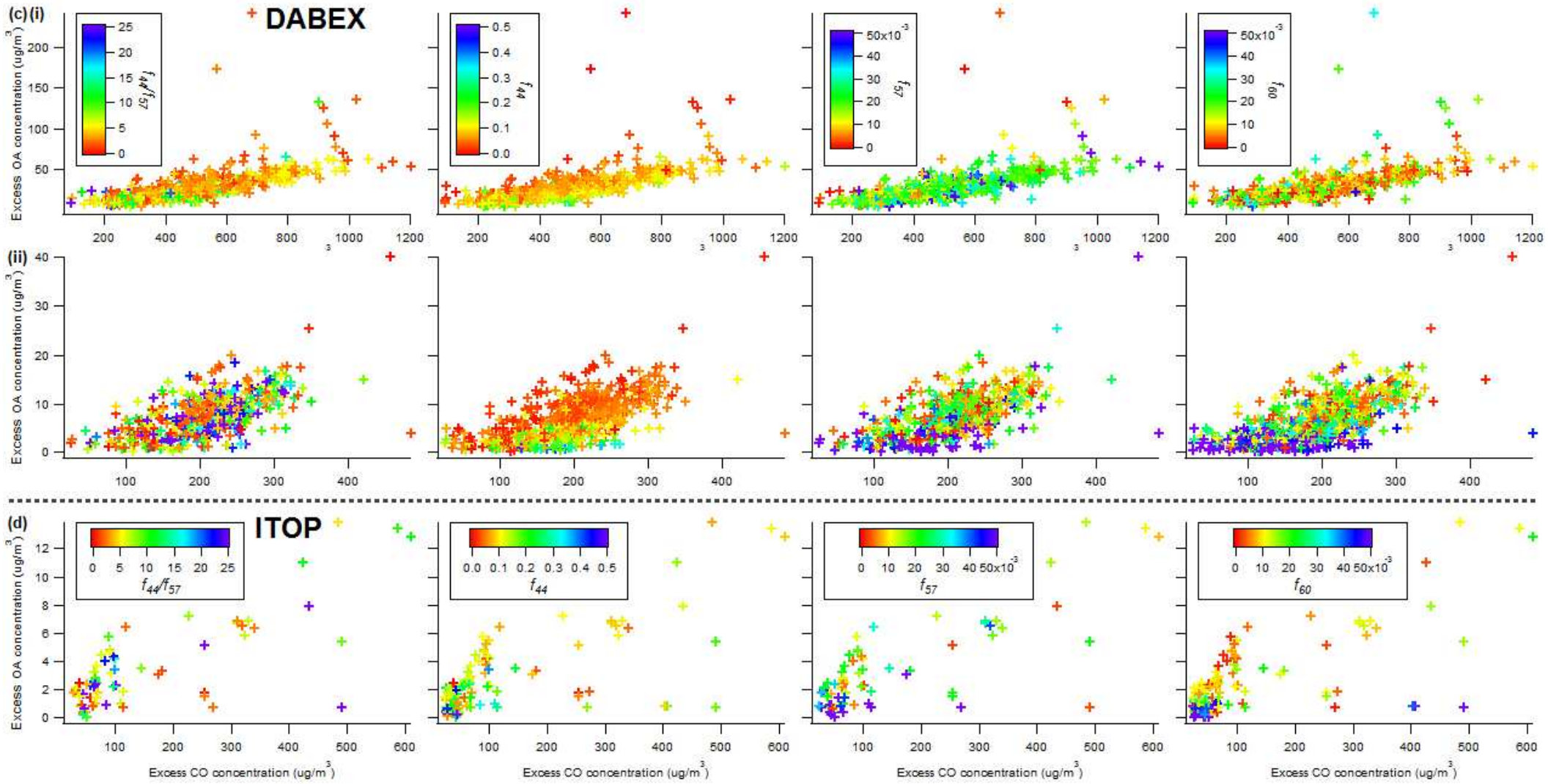
(c) (i)
DABEX
Excess OA concentration (ug/m3)
f44/f57
f44
f57
f60
(ii)
(d)
ITOP
Excess CO concentration (ug/m3)

References

(S1) Allen, G.; et al. Aerosol and trace-gas measurements in the Darwin area during the wet season. *J. Geophys. Res.-Atmos.* 2008, *113*, (D6).

(S2) Vaughan, G.; et al. SCOUT-03/ACTIVE - High-altitude aircraft measurements around deep tropical convection. *B. Am. Meteorol. Soc.* 2008, *89*, (5), 647-662.

(S3) Capes, G.; et al. Aging of biomass burning aerosols over West Africa: Aircraft measurements of chemical composition, microphysical properties, and emission ratios. *J. Geophys. Res.-Atmos.* 2008, *113*, (D20).

(S4) Haywood, J. M.; et al. Overview of the Dust and Biomass-burning Experiment and African Monsoon Multidisciplinary Analysis Special Observing Period-0. *J. Geophys. Res.-Atmos.* 2008, *113*.

(S5) Lewis, A. C.; et al. Chemical composition observed over the mid-Atlantic and the detection of pollution signatures far from source regions. *J. Geophys. Res.-Atmos.* 2007, *112*, (D10).

(S6) Fehsenfeld, F. C.; et al. International Consortium for Atmospheric Research on Transport and Transformation (ICARTT): North America to Europe - Overview of the 2004 summer field study. *J. Geophys. Res.-Atmos.* 2006, *111*, (D23).

(S7) Baumgardner, D.; et al. Physical and chemical properties of the regional mixed layer of Mexico's Megapolis. *Atmos. Chem. Phys.* 2009, *9*, (15), 5711-5727.

(S8) Molina, L. T.; et al. An overview of the MILAGRO 2006 Campaign: Mexico City emissions and their transport and transformation. *Atmos. Chem. Phys.* 2010, *10*, (18), 8697-8760.

(S9) Yokelson, R. J.; et al. Trace gas and particle emissions from open biomass burning in Mexico. *Atmos. Chem. Phys.* 2011, *11*, (14), 6787-6808.

(S10) Canagaratna, M. R.; et al. Chemical and microphysical characterization of ambient aerosols with the aerodyne aerosol mass spectrometer. *Mass Spectrom. Rev.* 2007, *26*, (2), 185-222.

(S11) Drewnick, F.; et al. Aerosol quantification with the Aerodyne Aerosol Mass Spectrometer: detection limits and ionizer background effects. *Atmos. Meas. Tech*. 2009, *2*, (1), 33–46.

(S12) Crosier, J.; et al. Chemical composition of summertime aerosol in the Po Valley (Italy), northern Adriatic and Black Sea. *Q. J. R. Meteorol. Soc*. 2007, *133*, (S1) 61–75.

(S13) Morgan, W. T.; et al. Vertical distribution of sub-micron aerosol chemical composition from North-Western Europe and the North-East Atlantic. *Atmos. Chem. Phys.* 2009, *9*, (15), 5389-5401.

(S14) Capes, G.; et al. Secondary organic aerosol from biogenic VOCs over West Africa during AMMA. *Atmos. Chem. Phys*. 2009, *9*, (12), 3841–3850.

(S15) Territory Natural Resource Management (TNRM) & Charles Darwin University Cooperative Research Centre for Tropical Savannas Management (CDU Tropical Savannas CRC). Northern Land Manager Tiwi Islands vegetation map, http://www.landmanager.org.au/ land_manager/downloads/Map-of-the-Vegetation-of-the-Tiwi-Islands-Region.pdf, September 2012.

(S16) TNRM & CDU Tropical Savannas CRC. Northern Land Manager Tiwi Islands vegetation map, http://www.landmanager.org.au/land_manager/downloads/Map-of-the-Vegetation-of-the-Darwin-Daly-Region.pdf, September 2012.

(S17) TNRM & CDU Tropical Savannas CRC. Northern Land Manager Tiwi Islands vegetation map, http://www.landmanager.org.au/land_manager/downloads/Map-of-the-Vegetation-of-the-Arnhem-Land.pdf, September 2012.

(S18) TNRM & CDU Tropical Savannas CRC. Northern Land Manager Tiwi Islands vegetation map, http://www.landmanager.org.au/land_manager/downloads/Map-of-the-Vegetation-of-the-Cape-York-Peninsula.pdf, September 2012.

(S19) Johnson, B. T.; et al. Aircraft measurements of biomass burning aerosol over West Africa during DABEX. *J. Geophys. Res.-Atmos.* 2008, *113*, (D17).

(S20) Fast, J. D.; et al. A meteorological overview of the MILAGRO field campaigns. *Atmos. Chem. Phys.* 2007, *7*, (9), 2233-2257.

(S21) Real, E.; et al. Processes influencing ozone levels in Alaskan forest fire plumes during long-range transport over the North Atlantic. *J. Geophys. Res.-Atmos.* 2007, *112*, (D10).

(S22) Petzold, A.; et al. Perturbation of the European free troposphere aerosol by North American forest fire plumes during the ICARTT-ITOP experiment in summer 2004. *Atmos. Chem. Phys.* 2007, *7*, (19), 5105-5127.